

# CATP: Context-Aware Trajectory Prediction with Competition Symbiosis

Jiang Wu  
Zhejiang University  
Hangzhou, China  
wujiang5521@zju.edu.cn

Dongyu Liu  
UC Davis  
Davis, CA, USA  
dyuliu@ucdavis.edu

Yuchen Lin  
Zhejiang University  
Hangzhou, China  
yuchenlin@zju.edu.cn

Yingcai Wu\*  
Zhejiang University  
Hangzhou, China  
ycwu@zju.edu.cn

## ABSTRACT

Contextual information is vital for accurate trajectory prediction. For instance, the intricate flying behavior of migratory birds hinges on their analysis of environmental cues such as wind direction and air pressure. However, the diverse and dynamic nature of contextual information renders it an arduous task for AI models to comprehend its impact on trajectories and consequently predict them accurately. To address this issue, we propose a “manager-worker” framework to unleash the full potential of contextual information and construct CATP model, an implementation of the framework for Context-Aware Trajectory Prediction. The framework comprises a manager model, several worker models, and a tailored training mechanism inspired by competition symbiosis in nature. Taking CATP as an example, each worker needs to compete against others for training data and develop an advantage in predicting specific moving patterns. The manager learns the workers’ performance in different contexts and selects the best one in the given context to predict trajectories, enabling CATP as a whole to operate in a symbiotic manner. We conducted two comparative experiments and an ablation study to quantitatively evaluate the proposed framework and CATP model. The results showed that CATP could outperform SOTA models, and the framework could be generalized to different context-aware tasks.

## CCS CONCEPTS

• **Computing methodologies** → **Machine learning algorithms**; *Neural networks*.

## KEYWORDS

context-aware trajectory prediction, training algorithm, ensemble learning

## ACM Reference Format:

Jiang Wu, Dongyu Liu, Yuchen Lin, and Yingcai Wu. 2018. CATP: Context-Aware Trajectory Prediction with Competition Symbiosis. In *Proceedings of Make sure to enter the correct conference title from your rights confirmation email (Conference acronym 'XX)*. ACM, New York, NY, USA, 16 pages. <https://doi.org/XXXXXXX.XXXXXXX>

\*Yingcai Wu is the corresponding author.

Permission to make digital or hard copies of all or part of this work for personal or classroom use is granted without fee provided that copies are not made or distributed for profit or commercial advantage and that copies bear this notice and the full citation on the first page. Copyrights for components of this work owned by others than the author(s) must be honored. Abstracting with credit is permitted. To copy otherwise, or republish, to post on servers or to redistribute to lists, requires prior specific permission and/or a fee. Request permissions from [permissions@acm.org](mailto:permissions@acm.org).

Conference acronym 'XX, June 03–05, 2018, Woodstock, NY

© 2018 Copyright held by the owner/author(s). Publication rights licensed to ACM.

ACM ISBN 978-1-4503-XXXX-X/18/06

<https://doi.org/XXXXXXX.XXXXXXX>

## 1 INTRODUCTION

Trajectory prediction is widely applied in many scenarios, such as traffic forecast [9, 22], pedestrians’ movements prediction [3], and sports player position prediction [21]. In most scenarios, contextual information can significantly affect the trajectories. For example, pedestrians will give way to each other and avoid obstacles [3]. Thus, many trajectory prediction models integrate contextual information to improve prediction accuracy.

However, as big data science evolves, contextual information has become diverse and dynamic, bringing new challenges. *Diversity*: The trajectory is affected by a combination of different types of contextual factors. For example, birds’ migratory trajectories are affected by wind direction, temperature, air pressure, etc. Multiple contextual factors collectively and interactively influence the trajectories. *Dynamic*: The contextual factors are ever-changing, leading to varied moving strategies and resulting trajectories. For example, birds may change their migratory routes as the wind directions change, since birds prefer to fly with a tailwind [19]. Video game players may change their trajectory when their opponents move to different places, to implement their counter competition plan.

Given such rich contextual information, AI models usually struggle to maximize its use to improve prediction accuracy, especially when we lack a large amount of labeled data recording how the contextual information affects trajectories. Models based on single components tailored for encoding contextual information (SC) [21, 22, 35] can accurately learn the impacts of contexts on trajectories. However, such models suffer from increasingly complex contextual characteristics [8]. Models based on ensemble learning (EL) [14, 18, 37] train multiple base learners on manually split sub-datasets and combine their results by weights, increasing prediction accuracy in diverse contexts. However, the performance of EL-based models depends heavily on how to split the dataset and assign weights reasonably, requiring a high level of domain expertise. Models based on reinforcement learning (RL) design rewards based on contexts and predict the trajectories that can gain the highest rewards. However, designing a reward function aligned with the predicted objects’ individual preferences for moving is challenging.

To tackle these challenges, we propose **CATP**, a **C**ontext-**A**ware **T**rajectory Prediction model. The innovation of CATP lies in the design of the **MW** framework, consisting of a **Manager** model, multiple **Worker** models, and a tailored training mechanism. Inspired by the two-part design of GAN [12] but unlike the two opposing parts in GAN, the manager and the workers are trained with competition symbiosis. We expect each worker to perform downstream tasks in specific contexts as accurately as possible (with competition), and the manager to select the most suitable worker in the given context to achieve high overall performance (with symbiosis). Taking CATP

as an example, multiple workers need to compete with each other for training data to develop their advantages in predicting trajectories with specific moving patterns. Meanwhile, the manager selects the best worker in the given context to perform trajectory prediction.

The MW framework can be further generalized to other tasks with context-awareness requirements. For example, we can adopt time-series forecasting models, such as TimesNet [32], as the workers to support context-aware traffic prediction. Each worker can learn the traffic patterns in certain contexts, and the manager can select the best worker based on contextual information like time, traffic lights, accidents, and weather conditions, etc.

We conducted three quantitative experiments to comprehensively evaluate CATP model and the MW framework. First, we compared CATP with SOTA models on context-aware trajectory prediction tasks. The results proved that our work outperformed the SOTA models, especially when the contextual information became complicated. Second, an ablation study further explored the performance of CATP under different model settings and training hyperparameters, to guide on training a robust CATP model. Third, we used sequential models as the worker and compared MW-based models with SOTA models on context-aware time-series prediction tasks, which proved the generalizability of the MW framework.

In summary, the contributions of this work are as follows:

- We propose the novel MW framework and the tailored training mechanism, which can be generalized to handling different context-aware tasks.
- We implement the proposed framework into context-aware trajectory prediction and develop the CATP model.
- We conducted two comparative experiments and an ablation study to comprehensively evaluate the effectiveness of CATP and the generalizability of the MW framework.

## 2 RELATED WORK

This work is most relevant to the context-aware prediction of trajectory data, or more generally, that of sequential data.

**SC-based models** were end-to-end – from contextual information and past trajectories to predicted trajectories – with specific components that could encode the contextual information [9, 15, 22, 35]. Such models inherited the strengths and limitations of end-to-end learning [11]. A well-trained model can accurately know the impacts of contextual information on trajectories. However, due to a lack of explainability and diagnosability, such models can be hard to train, especially when the data at both ends are complex.

Compared with these models, CATP **simplifies** the training process with the two-part model design. Each worker only learns specific moving patterns, without interactions with the complicated contextual information. The manager only selects the most suitable worker in the given context, rather than knowing the final trajectories. While it may not surpass a well-tuned single context-aware model in every instance, CATP has a greater potential for achieving optimal training outcomes.

**EL-based models** trained multiple basic trajectory prediction models and applied weights on the prediction results of each model, resulting in a final prediction [8, 14, 18, 31, 37]. Such models benefited from advanced techniques in adapting each basic model to a subset of training data [34]. However, there still exist two key

issues, namely, how to split the dataset to ensure each basic model is different and how to adjust the weights. Compared with existing methods, our method can automatically address these two issues in a data-driven manner.

For dataset partition, Jiang et al. [14] and Lin et al. [20] split the dataset from the spatial and temporal dimensions, respectively. Instead of splitting the dataset by specific rules constructed manually, CATP utilizes the manager model to filter the most suitable data samples for training each worker model.

For model weight adjustment, Li et al. [18] averaged the predictions of most models predicting the same direction by plurality voting. Fazla et al. [10] transferred side information into constraints on model weights. Le et al. [17] continuously deleted basic models (weight is 0) with high prediction loss and added new ones (weight is 1) to adapt to the context changes. Instead of combining the results of every base learner by weights, CATP allocates the most suitable worker for a specific trajectory prediction task.

**RL-based models** designed rewards based on contextual information and predicted the values that could gain the highest rewards [7, 24]. Thus, the results are quantifiable and thereby interpretable.

The premise of applying such models is that the subject to predict will move on the optimal path in most cases. For example, most car drivers follow the best routes provided by navigation APPs, which will be highly rewarded by RL-based models obviously. However, the subject may not always know which route is optimal in practice. For example, birds may be disturbed by some environmental factors and become disoriented during migration. Video game players may take diverse routes due to the uncertainty caused by not being able to observe the opponent's state at all times. In these cases, it is hard for RL-based methods to determine the reward functions. Compared to RL-based models, CATP is data-driven – workers learn the real moving patterns in the dataset, and the manager selects workers based on their performance – without relying on domain knowledge.

## 3 PRELIMINARIES

### 3.1 Data Description

Our study mainly considers two types of data, namely, trajectory data and context data. See the glossary table in Appendix A.

**Trajectory Data.** A trajectory of a unit  $u$  records the locations of  $u$  at certain moments. Given the current time  $t$ , we denote the past trajectory as  $T_{t,\Delta t,L}^u = (loc_{t-(L-1)\Delta t}^u, loc_{t-(L-2)\Delta t}^u, \dots, loc_t^u)$ , where  $\Delta t$  stands for the time interval between two consecutive records, and  $L$  is the length of the trajectory. Each location record  $loc_i^u$  in trajectory  $T_{t,\Delta t,L}^u$  is a coordinate (e.g., a 2D one can be  $loc_i^u = (x_i^u, y_i^u)$ ). Similarly, we denote the predicted trajectory after  $t$  as  $\hat{T}_{t+L\Delta t,\Delta t,L}^u = (\hat{loc}_{t+L\Delta t}^u, \hat{loc}_{t+L\Delta t+\Delta t}^u, \dots, \hat{loc}_{t+L\Delta t+L\Delta t}^u)$ , where  $\hat{loc}_i^u$  is the predicted location of  $u$  at time  $i$ .

**Context Data.** The context data records the latest observed data frames, denoted  $C_{t,\Delta t,L} = \{df_{t-(L-1)\Delta t}, df_{t-(L-2)\Delta t}, \dots, df_t\}$ , where each data frame  $df_t$  records  $N$  contextual data states (e.g., air pressure) at time  $t$ , denoted  $df_t = \{ds_t^1, ds_t^2, \dots, ds_t^N\}$ . To align different data states, we normalize each data state  $ds_t^i$  in our datasets based on their value types.

- **Ranged data state** is numerical data, of which the value must be in a specific range  $[MIN^i, MAX^i]$  (e.g., the time of day).

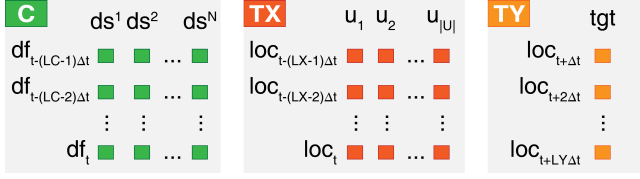


**Figure 1: A data sample consists of three parts, all in matrix form. The shapes of  $C$ ,  $TX$ , and  $TY$  are  $LC \times (N + \sum(LE^i - 1))$ ,  $LX \times 2|U|$ , and  $LY \times 2$ , respectively.**

Thus, we adopt a linear projection normalization function  $(ds_t^i - MIN^i)/(MAX^i - MIN^i)$ .

- **Unlimited data state** is also numerical data, of which the value starts from 0 and has no specific upper limit but only a “soft” upper limit  $\hat{MAX}^i$  (e.g., the wind speed). The data value will fall within  $[0, \hat{MAX}^i]$  in most cases (80% in this work). We normalize the unlimited data state by  $\tanh(ds_t^i/\hat{MAX}^i)$ , so that our model can adapt to most changes in the data state.
- **Boolean data state** is categorical data with two opposing states (e.g., daytime or nighttime). We simply use 0 for one state and 1 for the other.
- **Enumerated data state** is nominal data with discrete values (e.g., the bird type). In this work, enumerated data states with less than 10 categories are encoded by one-hot vectors. Others are encoded with shorter embedding vectors [23], which are trained along with CATP (see Section CATP), for the sake of saving memory.

### 3.2 Problem Formulation

The problem can be formulated as, given a set  $U$  of  $|U|$  units and a target object  $o \in U$ , our model attempts to predict the future trajectory of  $o$  based on the past trajectories of all units in  $U$ , with the assistance of the context data observed. Shown as Figure 1, the input consists of two parts, namely, the observed context data  $C = C_{t,\Delta t,LC}$  and a set of the past trajectories  $TX = \{T_{t,\Delta t,LX}^u | u \in U\}$ , where  $LC$  and  $LX$  are the number of data frames in context data and the length of past trajectories, respectively. Note that we also regard the past positions of all units as important contextual information, so we record them in both  $C$  and  $TX$ . Given  $C$  and  $TX$ , our model is expected to output the predicted trajectory of  $o$  after moment  $t$ , denoted  $\hat{TY} = \hat{T}_{t+LY\Delta t,\Delta t,LY}^o$ , where  $LY$  is the length of predicted trajectory. The predicted trajectory  $\hat{TY}$  should be as close as possible to the actual trajectory  $TY = T_{t+LY\Delta t,\Delta t,LY}^o$ .

## 4 CATP

This section outlines the model structure and training process of CATP, which is adaptable to models based on the MW framework for other context-aware tasks.

### 4.1 Modeling

CATP consists of a manager model  $M$  and  $K$  worker models from  $W_1$  to  $W_K$ , shown as Figure 2. First,  $M$  predicts the probability that each worker can accurately predict the trajectory in the context  $C$ . Then, the worker with the highest probability will be selected to predict  $\hat{TY}$  based on  $TX$ .

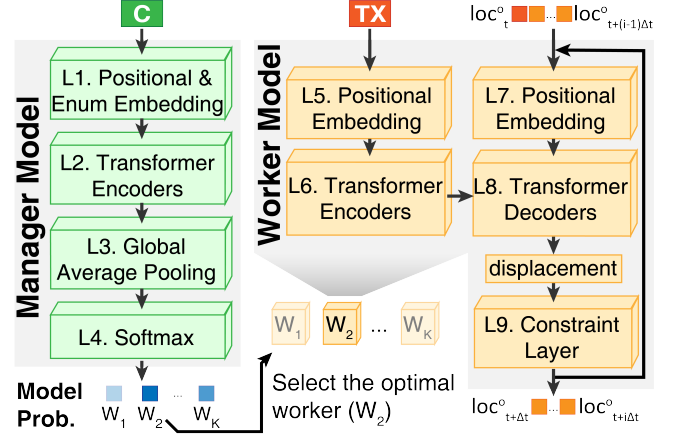


**Figure 2: CATP consists of a manager model (layers L1-L4) and multiple worker models (layers L5-L9). The manager selects the optimal worker in a given context  $C$ , and the selected worker predicts  $\hat{TY}$  based on  $TX$  accurately.**

**4.1.1 Manager model.** The manager model performs a  $K$  classification task, mapping the context data  $C$  to one of the  $K$  workers. Shown as Figure 2, the manager model is built based on the well-known Transformer model [13, 30], with sinusoidal positional embedding (L1) and 12 Transformer encoders (L2) by default. There exist two customized parts as follows. First, the embedding layer (L1) also encodes the enumerated data state in each  $df_t$ . Second, following the works using Transformer for classification tasks [6, 36], we add a Global Average Pooling layer (L3) and a Softmax layer (L4) to output a probability distribution over  $K$  classes.

**4.1.2 Worker model.** The selected worker model predicts  $\hat{TY}$  based on  $TX$ , shown as Figure 2. Our MW framework can accommodate any sequential prediction model as the worker model. CATP selects the Transformer model due to its excellent performance and widespread adoption across various domains [13, 28]. The model uses sinusoidal positional embedding (L5 and L7), 12 Transformer encoders (L6) learning the moving patterns in  $TX$ , and 12 decoders (L8) predicting the displacement at each  $\Delta t$  duration by default. The displacement between  $t + (i - 1)\Delta t$  and  $t + i\Delta t$ , denoted  $\hat{dis}_i$ , is predicted based on the start location  $loc_t^o$  and previous predicted trajectory from  $\hat{loc}_{t+\Delta t}^o$  to  $\hat{loc}_{t+(i-1)\Delta t}^o$ . To ensure the predicted trajectory is reasonable, we add a constraint layer (L9) to limit the Euclidean distance  $\|\hat{dis}_i\|_2$  not to exceed the maximum moving speed  $MaxMS$ :

$$\begin{aligned} scale &= \text{Sigmoid}(\|\hat{dis}_i\|_2) \times MaxMS / \|\hat{dis}_i\|_2, \\ \hat{loc}_{t+i\Delta t}^o &= \hat{loc}_{t+(i-1)\Delta t}^o + scale \times \hat{dis}_i. \end{aligned} \quad (1)$$

### 4.2 Training Mechanism

We propose an iterative training algorithm to train the manager and workers with competition symbiosis, shown as Figure 3 and Algorithm 1. **The competition** is reflected in that the workers need to compete with each other to be selected by the manager and gain more training data for advancement. **The symbiosis** is reflected in

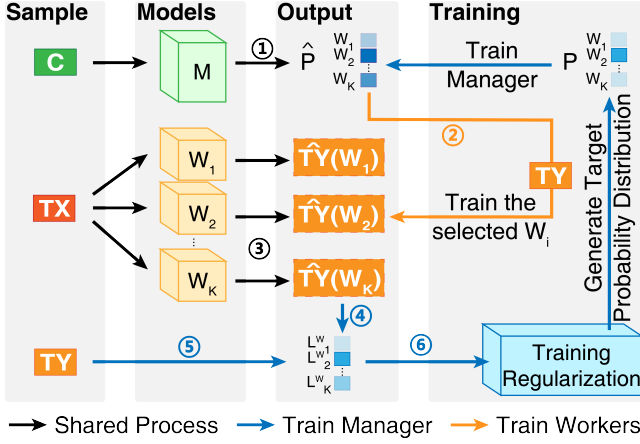


**Figure 3: The proposed training mechanism.** We first train workers based on the manager’s results and then train the manager based on workers’ performance.

that we use the results of the manager and workers to enhance each other to improve the overall performance of CATP. The main training process and some details are as follows.

**4.2.1 Main training process.** At each iteration, we first train the workers, shown as the black and orange arrows in Figure 3 and lines 4-15 in Algorithm 1. For each data sample, the manager firstly predicts a probability  $\hat{P}$  in context  $C$  (arrow ①). Then, only the worker  $W_i$  with the highest probability is trained (arrow ②), to predict  $\hat{T}Y$  based on  $TX$  (arrow ③), with  $TY$  as target. We expect to train each worker with data samples in specific contexts so that different workers can master the moving patterns in different contexts.

Then, we train the manager (the black and blue arrows in Figure 3 and lines 16-22 in Algorithm 1) to predict the probability distribution  $\hat{P}$  based on  $C$  (arrow ①). The key issue is to find the target probability distribution  $P$  because there exists no ground truth. A basic idea is that the worker with a low prediction loss should have a high probability of being selected. Thus, we use each worker to predict the trajectories (arrow ③) and obtain the prediction loss  $L_i^W$  of each model  $W_i$  (arrows ④-⑤). Based on each worker’s loss, we can construct the simplest target probability distribution  $P$  as a candidate:

$$\begin{aligned} \text{Max}L &= \max_{1 \leq i \leq K} L_i^W, \\ P &= \text{Softmax}\left(\frac{\text{Max}L}{L^W}\right). \end{aligned} \quad (2)$$

**Detail #1: training order.** We train the manager after the workers because the manager needs to learn about the workers’ performance. At the beginning of training, when the workers can hardly predict the trajectory, training the manager is meaningless.

**Detail #2: training regularization.** A key of training CATP is to balance the training of each worker. In a bad competition, as long as a worker  $W_i$  performs better than other workers, whether accurate or not, the manager tends to select it and assign more data samples to train  $W_i$  at the next iteration. In contrast, other workers, unable to improve due to lack of training data, are more difficult to be selected by the manager in the future. Finally, only one dominant worker is

**Algorithm 1** The iterative training process.

**Input:** training dataset  $D$ , the number of workers  $K$ , the number of steps for training manager  $T$ , and batch size  $b$

**Output:** a manager and  $K$  workers

```

1:  $M = \text{ManagerModel}(K)$ 
2:  $W_1, \dots, W_K = \text{WorkerModel}() \times K$ 
3: for number of training iterations do
4:   // Fix the manager and train the workers
5:   for  $\alpha$  steps do
6:      $S = \text{sample\_batch}(D, b)$ 
7:      $c, tx, ty = \text{parse}(S)$ 
8:      $\hat{P} = M(c)$ 
9:     for each worker  $W_i$  do
10:       $\text{sub\_batch} = []$ 
11:      for each sample  $s_j$  in  $S$  do
12:        if  $\hat{P}[j][i] == \max(\hat{P}[j])$  then
13:           $\text{sub\_batch.append}(s_j)$ 
14:        train  $W_i$  with trajectories in  $\text{sub\_batch}$ 
15:       $V_i += |\text{sub\_batch}|$ 
16:   // Fix the workers and train the manager
17:    $S = \text{sample\_batch}(D, b)$ 
18:    $c, tx, ty = \text{parse}(S)$ 
19:   for each worker  $W_i$  do
20:      $L_i^W = \text{ADE}(W_i(tx), ty)$ 
21:    $\text{model\_loss} = \text{Regularize}(L^W, V)$ 
22:   train  $M$  with  $\text{model\_loss}$ 
23: return  $M, W_1, \dots, W_K$ 

```

well trained and selected, resulting in a lack of model diversity and context data becoming useless.

Monte-Carlo Tree Search [5] (MCTS) faces a similar issue – whether to select the node with the highest winning rate or the ones without sufficient exploration. Inspired by MCTS, we add a training regularization term (arrow ⑥, line 21, Equation 3) to consider the training volume  $V_i$  – the number of data samples used to train each worker model  $W_i$  (line 15):

$$\begin{aligned} \text{Max}V &= \max_{1 \leq i \leq K} V_i, \\ P &= \text{Softmax}\left(e^{-\frac{L^W}{\text{Max}L}} + \beta \times \frac{\text{Max}V - V}{\text{Max}V}\right), \end{aligned} \quad (3)$$

where  $e^{-L^W/\text{Max}L}$  is the new loss term (TNewLoss), different from the one  $\text{Max}L/L^W$  in Equation 2 (TOriginLoss), and  $(\text{Max}V - V)/\text{Max}V$  is the regularization term (TReg).

For the regularization term, we expect it to be large at the beginning – so that each worker is sufficiently trained – and small at the end – so that the manager can accurately learn the workers’ performance. TReg satisfies our expectation because  $\text{Max}V$  usually increases faster than  $\text{Max}V - V$ , making TReg become small. Parameter  $\beta$  can also control the weight of TReg.

For the loss term, we change TOriginLoss to TNewLoss, since TReg ranges from 0 to 1, but TOriginLoss ranges from 1 to infinity, which may overshadow the impact of TReg on  $\hat{P}$ . In contrast, TNewLoss has a similar range ( $1/e$  to 1) to TReg, ensuring both terms can affect  $\hat{P}$ .

**Detail #3: batch training.** Figure 3 demonstrates how we train CATP with only one data sample, which may be easy to understand but not efficient. Actually, our algorithm supports batch training, shown as lines 5-15 in Algorithm 1. The key is that, given a batch of data samples, we split the batch into  $K$  sub-batches. For the  $i$ -th sub-batch, we require that worker  $W_i$  has the lowest loss on each data sample. We further train each worker  $W_i$  on the  $i$ -th sub-batch so that it better predicts trajectories occurring in the sub-batch. To ensure the workers are adequately trained, we repeatedly train the workers  $\alpha$  times (line 5) at each iteration.

**Detail #4: loss function selection.** For workers, there exist two widely used measures for evaluating the predicted trajectory, namely, the Average Displacement Error (ADE, Equation 4) and the Final Displacement Error (FDE, Equation 5). ADE computes the average L2 distance of all pairs of predicted and ground truth locations, while FDE computes the L2 distance of the final pair of locations. In this paper, we adopt ADE as the default loss function and denote the ADE loss of  $W_i$  as  $L_i^W$ .

$$ADE(TY, \hat{TY}) = \frac{\sum_{i=1}^{LY} \|\hat{loc}_{t+i\Delta t} - loc_{t+i\Delta t}\|_2}{LY} \quad (4)$$

$$FDE(TY, \hat{TY}) = \|\hat{loc}_{t+LY\Delta t} - loc_{t+LY\Delta t}\|_2 \quad (5)$$

For the manager, we adopt Wasserstein distance [2] (Equation 6) to compute the loss of  $\hat{P}$  from  $P$ . Compared to KL divergence and JS divergence, Wasserstein distance is continuous and differentiable, which can provide a linear gradient and prevent collapse mode.

$$\mathbb{W}(\hat{P}, P) = \sup_{\|f\|_L \leq 1} \mathbb{E}_{x \sim \hat{P}}[f(x)] - \mathbb{E}_{x \sim P}[f(x)], \quad (6)$$

where  $f(x)$  is required to be a 1-Lipschitz continuous function that satisfies  $|f(x_1) - f(x_2)| \leq |x_1 - x_2|$ , smoothing the loss function.

### 4.3 Full Objective

Our full objective is to minimize the prediction loss of the selected worker. However, the most selected trajectory may not be necessarily selected in a specific case. Thus, we propose top- $k$  loss – the minimum prediction loss of  $k$  workers with the highest probability. When using top- $k$  loss, our full objective is:

$$\text{minimize } \min_{1 \leq i \leq k} ADE(TY, W_{top_i}(TX)), \quad (7)$$

where  $top_i$  is the index number of the worker model with the  $i$ -th highest probability.

## 5 EVALUATION

We implemented CATP<sup>1</sup> and tested its performance by three quantitative experiments. Every model in our experiments was trained in three days on a server with an NVIDIA GeForce RTX 3090 Graphics Card (24 GB) using CUDA and PyTorch [27]. For each experiment, we performed a 10-round evaluation for each model over each dataset to compare model performance fairly (recorded in Appendix C). At each round, we re-sampled the dataset and re-trained the model.

**Table 1: Trajectory datasets used in Section 5.1.  $|S|$  is the number of data samples.**

Datasets	$ S $	$ U $	$N$	$\Delta t$	$LC/LX/LY$	$MaxMS$
DOTA	$10^5$	10	273	0.5s	5 / 30 / 10	275
Bird-8	7,000	1	8	300s	30 / 30 / 10	4km
Bird-2	7,000	1	2	300s	30 / 30 / 10	4km

### 5.1 Comparative Experiment I

In this experiment, we compared CATP with five context-aware trajectory prediction models over three datasets, to prove that CATP outperformed the SOTA context-aware trajectory prediction models. The experimental setup and results are shown as follows.

**5.1.1 Datasets.** We prepared three datasets, listed in Table 1. For each dataset, we put 80%, 10%, and 10% of data samples in the training, validation, and test set, respectively.

- DOTA is a dataset built on 1094 public DOTA 2 games on [25], which records players' trajectories and 273 contextual data status (e.g., the opponents' positions). We chose this dataset because the abundant contextual information helped us understand the capabilities and limitations of CATP. Since the virtual game has complex mechanisms, we designed tailored data sampling rules to obtain data samples with good quality. For example, we set  $LC = 5$  (smaller than  $LX$ ) because it may be difficult to learn the effects of excessive contextual information on trajectories. Details about the game and the dataset can be found in Appendix B).
- Bird-8 is based on an open bird migration dataset [16], which records the birds' migratory trajectories in a geographic coordinate system (leading the model loss to be calculated by spherical distance) and many contextual data states, from 2008 to 2019. We randomly sampled 7,000 trajectories and preserved eight contextual data states most relevant to trajectory prediction in Bird-8, e.g., the air temperature and the wind speed (see Appendix B).
- Bird-2 and Bird-8 are nearly identical, with only two contextual data states (i.e., the timestamp and the season). We set up this dataset to test our hypothesis that fewer contextual data states led to higher prediction loss.

**5.1.2 Models.** We compared four CATP variants with five baselines, including three SOTA ones.

**Baselines.** The five baselines are listed as follows.

- LSTM (vanilla LSTM). We concatenated  $TX$  and  $C$  at each time step and input the combined sequences into a model consisting of two LSTM layers with 128 units.
- Trans (vanilla Transformer). We adopted a model consisting of six transformer encoder layers and six transformer decoder layers, of which the embedding size was 128 and the input was the same as that for LSTM.
- DATF [26] is a SOTA single context-aware trajectory prediction model, which is capable of encoding multimodal contextual information and accepts both  $C$  and  $TX$  as input.
- Tjff (Trajformer [4]) is also a SOTA trajectory prediction model, which focuses on handling multiple agents' trajectories. Thus, Tjff accepts only  $TX$  as input, which can be regarded as an advanced alternative to our worker model.

<sup>1</sup>Code for anonymous review: <https://anonymous.4open.science/t/CATP-0710>

**Table 2: Results of Comparative Experiments I. We compared CATP with four baselines using the ADE loss (mean  $\pm$  sd).**

Model	Dataset		
	DOTA	Bird-8/km	Bird-2/km
LSTM	1279 $\pm$ 199	21.22 $\pm$ 3.06	23.41 $\pm$ 4.63
Trans	1227 $\pm$ 128	20.68 $\pm$ 2.76	24.42 $\pm$ 2.10
Tjf	969 $\pm$ 100	19.43 $\pm$ 1.95	19.43 $\pm$ 1.95
DATF	811 $\pm$ 116	15.90 $\pm$ 0.89	<b>16.64<math>\pm</math> 0.86</b>
IETP-10	625 $\pm$ 120	16.44 $\pm$ 0.81	20.27 $\pm$ 1.44
IETP-20	556 $\pm$ 49	13.78 $\pm$ 1.12	17.77 $\pm$ 1.64
CATP-10	563 $\pm$ 80	<b>11.94<math>\pm</math> 0.45</b>	17.74 $\pm$ 2.83
CATP-20	426 $\pm$ <b>33</b>	17.08 $\pm$ 1.41	23.31 $\pm$ 2.58
CATP-10-Tjf	538 $\pm$ 59	<b>11.94<math>\pm</math> 1.01</b>	17.26 $\pm$ 2.40
CATP-20-Tjf	<b>423<math>\pm</math> 39</b>	18.35 $\pm$ 1.80	21.22 $\pm$ 3.36

- IETP [18] is a SOTA EL-based method for context-aware trajectory prediction. We set its base learners as CATP’s worker model, to compare the mechanism of CATP (selecting the best worker) with that of EL (combining the results of all base learners). We reported the performance of IETP with 10 base learners (IETP-10) and 20 ones (IETP-20).

**Our model.** We reported the performance of four CATP variants, varying in the number of workers (CATP-10 or CATP-20) and whether to use Tjf as the worker (with or without Tjf suffixes). Detailed settings about CATP variants can be found in Section 5.2.

In order to ensure that all models were compared fairly, we added the same preprocessing layer (the enumerated data states embedding in our manager model) and post-process layer (the constraint layer in our worker model) to every model and trained them with a batch size of 64. The number of epochs was 30 with proper early stopping.

**5.1.3 Results.** We reported the top-1 ADE loss (MEAN) and the standard deviation (SD) in Table 2, which are analyzed as follows.

**CATP outperformed baselines especially when the context was complex.** CATP-20-Tjf and CATP-10 are clearly the winners on DOTA and Bird-8, respectively, where contextual information is richer. In contrast, DATF performed the best on Bird-2, but CATP-10 and CATP-10-Tjf was just slightly behind.

**Contextual information is crucial to trajectory prediction.** On all datasets, LSTM, Trans (which might underuse the contextual information), and Tjf (without C as input) had high ADE losses. Meanwhile, when predicting the bird migration trajectories, most models performed better on Bird-8 than on Bird-2, which meant that the contextual information facilitated trajectory prediction.

**Models with multiple base learners (CATP and IETP) tended to outperform single context-aware models (DATF) when context was complex.** DATF performed the best on Bird-2, while CATP-10 and IETP-20 outperformed DATF on others. These results suggested that a single model might struggle to learn an effective representation of complex contextual information and understand how it affected trajectories.

**Models with competition symbiosis (CATP) usually outperformed traditional EL-based models (IETP).** CATP models had a lower ADE loss than IETP on DOTA and Bird-8, respectively.

On Bird-2, CATP-10 achieved a similar accuracy as IETP. This indicated that the competition symbiosis enhanced CATP’s performance in diverse contexts.

**CATP can empower models to be context-aware.** The two transformer-based CATP models and the two with Tjf suffixes outperformed Trans and Tjf, respectively. It proved that CATP could significantly improve the performance of models without context-aware designs, even SOTA ones, by automatically splitting the dataset for each worker based on contextual information.

More comparison among multiple CATP variants can be found in Section 5.2, where we answered why CATP-10 performed better than CATP-20 on Bird dataset and how Tjf affected CATP’s performance as a worker.

## 5.2 Ablation Study

We conducted this study to better know the impacts of each key hyperparameter on CATP’s performance, thereby guiding how to build and train a robust CATP model.

**5.2.1 Training Traps.** Before analyzing the detailed results of each experimental group, we prefer to introduce two common training traps of CATP that occurred in many experimental groups. When CATP falls into these two traps, the manager model cannot work properly, leading the whole model to almost degenerate into a vanilla Transformer model.

- T1 One dominant worker was used in all contexts,** marked by  $\wedge$  in Table 3. When the regularization term had little effect on the training process, the manager tended to only select the worker with the lowest ADE loss and train it only, using it in all contexts. In this case, the manager’s accuracy is higher than 90%.
- T2 All workers were trained equally,** marked by  $\approx$  in Table 3. When the regularization term had an overweight effect on the training process, the manager tended to train each worker equally. Therefore, each worker could not learn unique moving patterns, and the manager could not know the suitable context for each worker, leading the manager’s accuracy to be lower than 20%.

The manager’s selection indicates what happened during the training process, helping model developers fine-tune the hyperparameters. For example, when the manager always selects the same worker, we can enhance the weight of the regularization term.

**5.2.2 Results.** After knowing the two training traps above, we elaborated the analysis of each experimental group as follows.

**Group A: a large  $K$  did not always result in lower prediction losses.** We changed  $K$  and  $\alpha$  correspondingly so that the number of data samples used to train each worker remains roughly the same. Due to the training regularization term, the manager model tends to use all worker models. However, when the number of worker models is small, one worker needs to learn many moving patterns, leading to high losses. When the number of worker models is large, many workers learn similar moving patterns and compete for the same training data, resulting in insufficient training data.

**Group B: competition symbiosis helps improve model performance.** We compared training algorithms with and without competition symbiosis (CSTrain) to examine its effects. For the one without CSTrain, we split the dataset randomly into  $K$  subsets, each for one



**Table 3: Results of ablation study.** There existed two control groups (CATP-10 and CATP-20) and seven experimental groups (from A to G), varying in the number of worker models ( $K$ ), whether to train with competition symbiosis (CSTrain), training parameters ( $\alpha$  and  $\beta$ ), the regularization function (Reg.), the loss functions (LossM and LossW), and the worker models (Worker). The empty cells were filled with the same settings of CATP-20. These model variations were evaluated by the top-1/top-3 ADE loss ( $MEAN \pm SD$ ) and manager accuracy (MngAcc, whether the top 3 workers had the lowest loss among all workers).

Group	$K$	CSTrain	$\alpha$	$\beta$	Reg.	LossM	LossW	Worker	Top-1 ADE	Top-3 ADE	MngAcc
CATP-20	20	✓	100	0.1	Eq. 3	Wasserstein	ADE	Transformer-based	426± 33	375± 28	81%
CATP-10	10	✓	50						564± 81	483± 65	83%
A	1 30		5 150						1228± 129 453± 28	/ 392± 25	100% $\wedge$ 75%
B		✗							1104± 106	1029± 91	8% $\approx$
C			1 500						983± 82 554± 47	910± 77 521± 40	10% $\approx$ 86%
D				0 1					1054± 91 879± 72	958± 83 844± 67	93% $\wedge$ 12% $\approx$
E					Eq. 2 Eq. 8				941± 124 793± 110	883± 105 714± 96	98% $\wedge$ 94% $\wedge$
F						Cross Entropy	FDE		603± 53 502± 47	539± 48 474± 39	62% 77%
G								Trajformer [4]	423± 39	362± 23	83%

worker. After all the workers finished training, we trained the manager model based on the workers' performance. Without CSTrain, the workers were trained equally, leading CATP to fall into Trap T2.

**Group C:  $\alpha$  should be fine-tuned during training.** When  $\alpha = 1$ , each worker obtained insufficient training data at each iteration and could not quickly converge at the beginning of training. Meanwhile, since every worker has a large loss, the manager model mainly relied on the regularization term, falling into Trap T2. A large  $\alpha$  makes workers converge quickly but eventually causes them to overfit. It is better to start with a large  $\alpha$  and keep reducing it.

**Group D:  $\beta$  is crucial for avoiding the two traps.** When  $\beta$  was zero, the manager model completely relies on the loss, falling into Trap T1. In contrast, when  $\beta$  was one, the manager model relied more on the training counts, falling into Trap T2.

**Group E: appropriate regularization functions help avoid Trap T1.** We tested two more regularization functions. One was Equation 2, which had no training regularization term. The other was Equation 8, which directly added a regularization term to Equation 2, without normalizing the loss term into  $[0, 1]$ . Both of these two regularization functions led CATP to fall into Trap T1.

$$P = \text{Softmax}\left(\frac{\text{Max}L}{L^W} + \beta \times \frac{\text{Max}V - V}{\text{Max}V}\right) \quad (8)$$

**Group F: loss functions affect model accuracy.** We tested cross entropy and FDE as the loss functions for training the manager model and worker models, respectively. Cross entropy underperformed Wasserstein loss, probably because Wasserstein loss allows the manager to converge quickly and consistently. FDE loss undoubtedly caused a higher ADE loss, but also a lower manager accuracy, probably because two moving strategies with the same destination,

but different trajectories were regarded as the same. Thus, many workers had to learn similar moving patterns, similar to the issue when setting  $K$  to 30 in Group A.

**Group G: CATP supports continuous performance improvement with SOTA model integration.** We replaced each worker model with Tjff and observed lower losses and a higher manager accuracy. It proved that workers' better performance can benefit the training of the manager and the overall performance.

### 5.3 Comparative Experiment II

This experiment was conducted to prove the generalizability of the MW framework. We adopted time-series prediction models as the workers to conduct context-aware time-series prediction tasks. The experimental setup and results are as follows.

**5.3.1 Datasets.** We tested our model on two open datasets, listed as follows and in Table 4.

- SP<sup>2</sup> is a dataset recording solar power data in 2006, with six contextual variables. We trained the models using the data in California and New York to ensure different changing patterns.
- ET<sup>3</sup> is a dataset used as a benchmark by many recent models. We trained the models on the subset named "ETT-h1" because of its rich contextual information. We set oil temperature (OT) as the target channel and used the other eight channels as the contexts.

To obtain sufficient data samples, we used different lengths of stride and time windows for data sampling, depending on the total length of the time series. The data sampling proportions in the training, validation, and test sets are 80%, 10%, and 10% respectively.

<sup>2</sup>Solar Power: <https://www.nrel.gov/grid/solar-power-data.html>

<sup>3</sup>ET: <https://github.com/zhouhaoyi/ETDataset>

**Table 4: Two time-series datasets used in Section 5.3. We obtained  $|S|$  data samples from  $Num$  original temporal sequences with length  $Len$ , at a certain Stride.**

Datasets	$Len \times Num$	Stride	$ S $	$N$	$LC/LX/LY$
SP	$105,120 \times 2$	12	17,490	5	96/96/96
ET	$17,420 \times 1$	10	1,731	8	60/60/60

**5.3.2 Models.** We compared three CATP variants with six time-series prediction models, including four SOTA ones. All these models were trained with a batch size of 32. The number of epochs was set to 8 with proper early stopping.

**Baselines.** The first two baselines were LSTM and Trans, which were also used in Comparative Experiment I. We also selected four SOTA models – Informer [38], Autoformer [33], FEDFormer [39], and TimesNet [32]. Since these baselines have no components for contextual channels, we concatenated the contextual channels and the target channel to construct multivariate time-series data as the input of these baseline models. Based on such considerations, we did not select models designed to handle univariate time-series data as our baselines (e.g., ARIMA [1] and DeepAR [29]).

**Our model.** We replaced the workers with time-series prediction models, namely, LSTM, Trans, and TimesNet, and built MW-LSTM, MW-Trans, and MW-TN, respectively. In contrast to the baselines, we used the contextual channels and the to-be-predicted channel as the input of manager and workers, respectively, so that we can highlight the capabilities and limitations of the MW framework. Considering the complexity of each dataset, we set the number of workers to 10, 20, and 15 for MSL, SP, and ET, respectively. Other hyperparameters were set to the optimal values tested in our Ablation Study (Section 5.2).

**5.3.3 Results.** We reported the top-1 MSE loss ( $MSE = \frac{1}{n} \sum_{i=1}^n (y - \hat{y})^2$ ) in Table 5, which proved that the MW framework could be applied to other context-aware tasks. Here are detailed analysis. **1) The MW framework could significantly improve the performance of simple models.** MW-LSTM and MW-Trans outperformed LSTM and Trans and achieved a similar accuracy as Informer. **2) The MW framework and SOTA models were mutually beneficial.** MW-TN achieved better performance than both TimesNet and other MW-based models. The framework provided a better training set for SOTA models, while SOTA models enhanced the performance of the model as a whole.

## 6 DISCUSSION

**Generalizability.** Although CATP mainly focuses on trajectory prediction, the MW framework – the core contributions of our research – can be generalized to many context-aware tasks. The MW framework essentially provides a data-driven method to automatically split the training dataset based on contextual factors and workers’ performances. Such a method uses the manager model to perceive contextual information and allows the replaceable workers to focus only on downstream tasks. Meanwhile, using SOTA models as the worker could enhance the overall model performance, resulting in continuous improvement on CATP as the SOTA models evolve.

**Table 5: Results of Comparative Experiment II. We compared our model with six baselines using the MSE loss (MEAN  $\pm$  SD).**

Model	Dataset	
	SP	ET
LSTM	5.69 $\pm$ 0.54	1.40 $\pm$ 0.12
Trans	5.57 $\pm$ 0.63	1.23 $\pm$ 0.13
Informer	4.81 $\pm$ 0.81	1.04 $\pm$ 0.12
Autoformer	3.16 $\pm$ 0.31	0.50 $\pm$ 0.05
FEDFormer	3.16 $\pm$ 0.32	0.46 $\pm$ 0.05
TimesNet	2.93 $\pm$ 0.23	0.47 $\pm$ 0.05
MW-LSTM	4.86 $\pm$ 0.39	0.99 $\pm$ 0.10
MW-Trans	4.74 $\pm$ 0.56	1.00 $\pm$ 0.11
MW-TN	<b>2.86<math>\pm</math>0.13</b>	<b>0.45<math>\pm</math>0.04</b>

**Why the MW framework.** Increasingly dynamic and complex contextual information results in inefficiencies for a single model to fully leverage such information. As outlined in our Introduction and Related Work sections, ensemble methods are outperforming single-model approaches. The main challenge with ensemble methods is the considerable effort and expertise required to partition training samples so that the “workers” can effectively learn the intended knowledge. Our solution automates this process, enabling the “manager” to allocate the most appropriate training data to each worker and harness the potential of existing sequential models. The experimental results confirm our design’s efficacy.

**Limitations and future works.** The number of worker models is highly dependent on the variety of trajectories to predict in different contexts. We usually need to fine-tune this hyperparameter and re-train the whole model when the trajectory patterns change (e.g., when applying to a new application). In the future, we plan to study how to automatically and progressively fine-tune the number of workers. One possible solution is to allow the manager to retire underperforming workers and bring in new ones during training. It is also a promising solution to use some pre-trained models as the workers and allow the manager to fine-tune them quickly.

## 7 CONCLUSION

We introduced a context-aware trajectory prediction model, which could effectively use complex contextual information to improve prediction accuracy. Similar to the GAN networks, our proposed model consisted of several worker models for predicting trajectory and a manager model for selecting the best worker model in the given context. We further proposed a training mechanism with competition symbiosis, where the results of the manager and the workers could be used to train each other, and the workers with lower prediction losses can gain more training data to perform better in specific contexts. We conducted two comparative experiments to evaluate the performance and generalizability of CATP, where CATP effectively improved the prediction accuracy of both trajectory and time-series data, especially when the context data is complex. An ablation study further evaluated the performance of several model variations and provided guidance on how to train a robust CATP model.



## REFERENCES

- [1] Adebisi A. Ariyo, Adewumi O. Adewumi, and Charles K. Ayo. 2014. Stock Price Prediction Using the ARIMA Model. In *2014 UKSim-AMSS 16th International Conference on Computer Modelling and Simulation*. 106–112. <https://doi.org/10.1109/UKSim.2014.67>
- [2] Martin Arjovsky, Soumith Chintala, and Léon Bottou. 2017. Wasserstein Generative Adversarial Networks. In *Proceedings of the 34th International Conference on Machine Learning*, Vol. 70. PMLR, 214–223. <https://proceedings.mlr.press/v70/arjovsky17a.html>
- [3] Federico Bartoli, Giuseppe Lisanti, Lamberto Ballan, and Alberto Del Bimbo. 2018. Context-Aware Trajectory Prediction. In *24th International Conference on Pattern Recognition (ICPR)*. 1941–1946. <https://doi.org/10.1109/ICPR.2018.8545447>
- [4] Manoj Bhat, Jonathan Francis, and Jean Oh. 2020. Trajformer: Trajectory Prediction with Local Self-Attentive Contexts for Autonomous Driving. <https://doi.org/10.48550/arXiv.2011.14910> [cs.CV]
- [5] Cameron B. Browne, Edward Powley, Daniel Whitehouse, Simon M. Lucas, Peter I. Cowling, Philipp Rohlfshagen, Stephen Tavener, Diego Perez, Spyridon Samothracis, and Simon Colton. 2012. A Survey of Monte Carlo Tree Search Methods. *IEEE Transactions on Computational Intelligence and AI in Games* 4, 1 (2012), 1–43. <https://doi.org/10.1109/TCIAIG.2012.2186810>
- [6] Chun-Fu Richard Chen, Quanfu Fan, and Rameswar Panda. 2021. CrossViT: Cross-Attention Multi-Scale Vision Transformer for Image Classification. In *IEEE/CVF International Conference on Computer Vision (ICCV)*. 347–356. <https://doi.org/10.1109/ICCV48922.2021.00041>
- [7] John Co-Reyes, YuXuan Liu, Abhishek Gupta, Benjamin Eysenbach, Pieter Abbeel, and Sergey Levine. 2018. Self-consistent trajectory autoencoder: Hierarchical reinforcement learning with trajectory embeddings. In *International conference on machine learning*. PMLR, 1009–1018. <https://doi.org/10.48550/arXiv.1806.02813>
- [8] Xibin Dong, Zhiwen Yu, Wenming Cao, Yifan Shi, and Qianli Ma. 2020. A survey on ensemble learning. *Frontiers of Computer Science* 14 (2020), 241–258. <https://doi.org/10.1007/s11704-019-8208-z>
- [9] Ziquan Fang, Lu Pan, Lu Chen, Yuntao Du, and Yunjun Gao. 2021. MDTP: A Multi-Source Deep Traffic Prediction Framework over Spatio-Temporal Trajectory Data. *Proc. VLDB Endow.* 14, 8 (apr 2021), 1289–1297. <https://doi.org/10.14778/3457390.3457394>
- [10] Arda Fazla, Mustafa Enes Aydin, Orhun Tamyigit, and Suleyman Serdar Kozat. 2022. Context-Aware Ensemble Learning for Time Series. <https://doi.org/10.48550/arXiv.2211.16884>
- [11] Tobias Glasmachers. 2017. Limits of end-to-end learning. In *Asian conference on machine learning*. PMLR, 17–32. <https://doi.org/10.48550/arXiv.1704.08305>
- [12] Ian Goodfellow, Jean Pouget-Abadie, Mehdi Mirza, Bing Xu, David Warde-Farley, Sherjil Ozair, Aaron Courville, and Yoshua Bengio. 2020. Generative Adversarial Networks. *Commun. ACM* 63, 11 (2020), 139–144. <https://doi.org/10.1145/3422622>
- [13] Kai Han, An Xiao, Enhua Wu, Jianyuan Guo, Chunjing XU, and Yunhe Wang. 2021. Transformer in Transformer. 34 (2021), 15908–15919. [https://proceedings.neurips.cc/paper\\_files/paper/2021/file/854d9fca60b4bd07f9bb215d59ef5561-Paper.pdf](https://proceedings.neurips.cc/paper_files/paper/2021/file/854d9fca60b4bd07f9bb215d59ef5561-Paper.pdf)
- [14] Zhe Jiang, Yan Li, Shashi Shekhar, Lian Rampi, and Joseph Knight. 2017. Spatial Ensemble Learning for Heterogeneous Geographic Data with Class Ambiguity: A Summary of Results. In *Proceedings of the 25th ACM SIGSPATIAL International Conference on Advances in Geographic Information Systems*. Association for Computing Machinery, Article 23. <https://doi.org/10.1145/3139958.3140044>
- [15] Yilun Jin, Kai Chen, and Qiang Yang. 2022. Selective Cross-City Transfer Learning for Traffic Prediction via Source City Region Re-Weighting. In *Proceedings of the 28th ACM SIGKDD Conference on Knowledge Discovery and Data Mining*. Association for Computing Machinery, 731–741. <https://doi.org/10.1145/3534678.3539250>
- [16] B. Kranstauber, Hans van Gasteren, W. Bouten, and J.Z. Shamoun. 2022. Dataset for predictive bird migration model. (5 2022). <https://doi.org/10.21942/uva.19416215.v1>
- [17] Yann-Aël Le Borgne, Silvia Santini, and Gianluca Bontempi. 2007. Adaptive model selection for time series prediction in wireless sensor networks. *Signal Processing* 87, 12 (2007), 3010–3020. <https://doi.org/10.1016/j.sigpro.2007.05.015> Special Section: Information Processing and Data Management in Wireless Sensor Networks.
- [18] Zirui Li, Yunlong Lin, Cheng Gong, Xinwei Wang, Qi Liu, Jianwei Gong, and Chao Lu. 2022. An Ensemble Learning Framework for Vehicle Trajectory Prediction in Interactive Scenarios. In *IEEE Intelligent Vehicles Symposium (IV)*. 51–57. <https://doi.org/10.1109/IV51971.2022.9827070>
- [19] Felix Liechti, Anders Hedenström, and Thomas Ålerstam. 1994. Effects of Sidewinds on Optimal Flight Speed of Birds. *Journal of Theoretical Biology* 170, 2 (1994), 219–225. <https://doi.org/10.1006/jtbi.1994.1181>
- [20] Ziqian Lin, Jie Feng, Ziyang Lu, Yong Li, and Depeng Jin. 2019. DeepSTN+: Context-Aware Spatial-Temporal Neural Network for Crowd Flow Prediction in Metropolis. *Proceedings of the AAAI Conference on Artificial Intelligence* 33, 1 (2019), 1020–1027. <https://doi.org/10.1609/aaai.v33i01.33011020>
- [21] Per Lindström, Ludwig Jacobsson, Niklas Carlsson, and Patrick Lambrix. 2020. Predicting player trajectories in shot situations in soccer. In *Machine Learning and Data Mining for Sports Analytics*. Springer International Publishing, 62–75. [https://doi.org/10.1007/978-3-030-64912-8\\_6](https://doi.org/10.1007/978-3-030-64912-8_6)
- [22] Yuhuan Lu, Wei Wang, Xiping Hu, Pengpeng Xu, Shengwei Zhou, and Ming Cai. 2022. Vehicle Trajectory Prediction in Connected Environments via Heterogeneous Context-Aware Graph Convolutional Networks. *IEEE Transactions on Intelligent Transportation Systems* (2022), 1–13. <https://doi.org/10.1109/TITS.2022.3173944>
- [23] Tomas Mikolov, Ilya Sutskever, Kai Chen, Greg S Corrado, and Jeff Dean. 2013. Distributed Representations of Words and Phrases and their Compositionality. In *Advances in Neural Information Processing Systems*, C.J. Burges, L. Bottou, M. Welling, Z. Ghahramani, and K.Q. Weinberger (Eds.), Vol. 26. Curran Associates, Inc. [https://proceedings.neurips.cc/paper\\_files/paper/2013/file/9aa42b31882ec039965f3c4923ce901b-Paper.pdf](https://proceedings.neurips.cc/paper_files/paper/2013/file/9aa42b31882ec039965f3c4923ce901b-Paper.pdf)
- [24] Stephanie Milani, Arthur Juliani, Ida Momennejad, Raluca Georgescu, Jaroslaw Rzepecki, Alison Shaw, Gavin Costello, Fei Fang, Sam Devlin, and Katja Hofmann. 2023. Navigates Like Me: Understanding How People Evaluate Human-Like AI in Video Games. In *Proceedings of the 2023 CHI Conference on Human Factors in Computing Systems*. 1–18. <https://doi.org/10.1145/3544548.3581348>
- [25] OpenDOTA. Feb. 2, 2023 – March. 3, 2023. <https://www.opendota.com/>
- [26] Seong Hyeon Park, Gyubok Lee, Jimin Seo, Manoj Bhat, Minseok Kang, Jonathan Francis, Ashwin Jadhav, Paul Pu Liang, and Louis-Philippe Morency. 2020. Diverse and Admissible Trajectory Forecasting Through Multimodal Context Understanding. In *Computer Vision – ECCV*. Springer, 282–298. [https://doi.org/10.1007/978-3-030-58621-8\\_17](https://doi.org/10.1007/978-3-030-58621-8_17)
- [27] Adam Paszke, Sam Gross, Francisco Massa, Adam Lerer, James Bradbury, Gregory Chanan, Trevor Killeen, Zeming Lin, Natalia Gimelshein, Luca Antiga, Alban Desmaison, Andreas Kopf, Edward Yang, Zachary DeVito, Martin Raison, Alykhan Tejani, Sasank Chilamkurthy, Benoit Steiner, Lu Fang, Junjie Bai, and Soumith Chintala. 2019. PyTorch: An Imperative Style, High-Performance Deep Learning Library. In *Advances in Neural Information Processing Systems*, Vol. 32. Curran Associates, Inc. [https://proceedings.neurips.cc/paper\\_files/paper/2019/file/bdbca288fee7f92f2bfa9f7012727740-Paper.pdf](https://proceedings.neurips.cc/paper_files/paper/2019/file/bdbca288fee7f92f2bfa9f7012727740-Paper.pdf)
- [28] Huimin Ren, Sijie Ruan, Yanhua Li, Jie Bao, Chuishi Meng, Ruiyuan Li, and Yu Zheng. 2021. MTrajRec: Map-Constrained Trajectory Recovery via Seq2Seq Multi-task Learning. In *Proceedings of the 27th ACM SIGKDD Conference on Knowledge Discovery & Data Mining*. Association for Computing Machinery, 1410–1419. <https://doi.org/10.1145/3447548.3467238>
- [29] David Salinas, Valentin Flunkert, Jan Gasthaus, and Tim Januschowski. 2020. DeepAR: Probabilistic forecasting with autoregressive recurrent networks. *International Journal of Forecasting* 36, 3 (2020), 1181–1191. <https://doi.org/10.1016/j.ijforecast.2019.07.001>
- [30] Ashish Vaswani, Noam Shazeer, Niki Parmar, Jakob Uszkoreit, Llion Jones, Aidan N Gomez, Łukasz Kaiser, and Illia Polosukhin. 2017. Attention is All you Need. 30 (2017). [https://proceedings.neurips.cc/paper\\_files/paper/2017/file/3f5ee243547dee91fbd053c1c4a845aa-Paper.pdf](https://proceedings.neurips.cc/paper_files/paper/2017/file/3f5ee243547dee91fbd053c1c4a845aa-Paper.pdf)
- [31] Ding Wang and Pang-Ning Tan. 2021. JOHAN: A Joint Online Hurricane Trajectory and Intensity Forecasting Framework. In *Proceedings of the 27th ACM SIGKDD Conference on Knowledge Discovery & Data Mining*. Association for Computing Machinery, 1677–1685. <https://doi.org/10.1145/3447548.3467400>
- [32] Haixu Wu, Tengge Hu, Yong Liu, Hang Zhou, Jianmin Wang, and Mingsheng Long. 2022. TimesNet: Temporal 2d-variation modeling for general time series analysis. *arXiv preprint arXiv:2210.02186* (2022). <https://doi.org/10.48550/arXiv.2210.02186>
- [33] Haixu Wu, Jiehui Xu, Jianmin Wang, and Mingsheng Long. 2021. Autoformer: Decomposition transformers with auto-correlation for long-term series forecasting. *Advances in Neural Information Processing Systems* 34 (2021), 22419–22430. <https://doi.org/10.48550/arXiv.2106.13008>
- [34] Yuan Xu, Jiajie Xu, Jing Zhao, Kai Zheng, An Liu, Lei Zhao, and Xiaofang Zhou. 2022. MetaPTP: An Adaptive Meta-optimized Model for Personalized Spatial Trajectory Prediction. In *Proceedings of the 28th ACM SIGKDD Conference on Knowledge Discovery and Data Mining*. Association for Computing Machinery, 2151–2159. <https://doi.org/10.1145/3534678.3539360>
- [35] Jian Yu, Meng Zhou, Xin Wang, Guoliang Pu, Chengqi Cheng, and Bo Chen. 2021. A dynamic and static context-aware attention network for trajectory prediction. *ISPRS International Journal of Geo-Information* 10, 5 (2021), 336. <https://doi.org/10.3390/ijgi10050336>
- [36] Hao Zhang, Yanbin Hao, and Chong-Wah Ngo. 2021. Token Shift Transformer for Video Classification. In *Proceedings of the 29th ACM International Conference on Multimedia*. Association for Computing Machinery, 917–925. <https://doi.org/10.1145/3474085.3475272>
- [37] Xiaocai Zhang, Zhixun Zhao, Yi Zheng, and Jinyan Li. 2020. Prediction of Taxi Destinations Using a Novel Data Embedding Method and Ensemble Learning. *IEEE Transactions on Intelligent Transportation Systems* 21, 1 (2020), 68–78. <https://doi.org/10.1109/TITS.2018.2888587>

- [38] Haoyi Zhou, Shanghang Zhang, Jieqi Peng, Shuai Zhang, Jianxin Li, Hui Xiong, and Wancai Zhang. 2021. Informer: Beyond efficient transformer for long sequence time-series forecasting. In Proceedings of the AAAI conference on artificial intelligence, Vol. 35. 11106–11115. <https://doi.org/10.48550/arXiv.2012.07436>
- [39] Tian Zhou, Ziqing Ma, Qingsong Wen, Xue Wang, Liang Sun, and Rong Jin. 2022. FEDformer: Frequency enhanced decomposed transformer for long-term series forecasting. In International Conference on Machine Learning. PMLR, 27268–27286. <https://doi.org/10.48550/arXiv.2201.12740>

## A GLOSSARY TABLE

**Table 6: Glossary Table.**

Symbol	Description	Note
<b>Input and Output</b>		
$TX$	the past trajectories of all recorded game units in $U$	$\{T_{t,\Delta t,LX}^u   u \in U\}$
$C$	the context data	$C_{t,\Delta t,LC}$
$TY$	the real trajectory of the player to predict after $t$	$T_{t+LY\Delta t,\Delta t,LY}^p$
$\hat{TY}$	the predicted trajectory of the player to predict after $t$	$\hat{T}_{t,\Delta t,LY}^p$
<b>Data-Related Symbols</b>		
$t$	a time point	
$\Delta t$	the time interval of data capturing	1 sec
$C_{t,\Delta t,L}$	the context data consisting of the latest $L$ data frames observed by $p$	$(df_{t-(L-1)\Delta t}, \dots, df_t)$
$df_t$	the data frame when observing the game at time $t$ , consisting of $N$ data states	$(ds_t^1, \dots, ds_t^N)$
$ds_t^i$	the $i$ -th data state in data frame $df_t$	
$T_{t,\Delta t,L}^u$	the trajectory of $u$ consisting of the latest $L$ locations	$(loc_{t-(L-1)\Delta t}^u, \dots, loc_t^u)$
$\hat{T}_{t+L\Delta t,\Delta t,L}^u$	the predicted trajectory of $u$ consisting of the next $L$ locations	$(loc_{t+\Delta t}^u, \dots, loc_{t+L\Delta t}^u)$
$u \in U$	a set of game units whose trajectories are recorded	
$p$	the player to predict	$p \in U$
$loc_t^u$	the 2D coordinate of $u$ at time $t$	$(x_t^u, y_t^u)$
$s$	a sample	$(C, TX, TY)$
$S$	a batch of samples	$(s_1, \dots, s_{ S })$
$LC$	the number of data frames in context data	5
$LX$	the length of past trajectories	30
$LY$	the length of the trajectories to predict	10
<b>Model-Related Symbols</b>		
$K$	the number of worker models	20
$k$	the top- $k$ worker models used to evaluate the model	3
$L$	the loss of the whole model	
$M$	the manager model	
$\hat{P}$	the probability of each model selected by the manager model	
$L^M$	the loss of the manager model	
$W_i$	the $i$ -th worker model	
$V_i$	the training volume of $W_i$	
$L_i^W$	the loss of the $i$ -th worker model	
$\hat{TY}_i$	$\hat{TY}$ of the $i$ -th worker model	

## B DATASETS

### B.1 DOTA

**B.1.1 Introduction to the Game.** DOTA 2 is a typical MOBA (Multiplayer Online Battle Arena) game. Two teams, each with five players, need to compete against each other on a well-designed map. To achieve effective teamwork in a highly competitive game, the players usually need to make competition plans based on the game context, and the competition plans require players to move to certain places on the map. For example, when an allied tower (a type of building) is about to be destroyed by the opponents (the contextual information), the players may move to the tower to protect it (the trajectories). A full introduction can be found on the wiki page: <https://dota2.fandom.com/>.

**Why this dataset?** Video games are becoming a new arena for researchers to gain a better understanding of the capabilities and limitations of AI, for many reasons:

- **High Data Volume.** A popular video game, such as PUBG and LOL, may have tens of millions of players. These players can generate a vast amount of game data every day. These data can be adequate for training a deep neural network optimally. We can get access to public data on OpenDOTA [25], an open-source DOTA 2 data platform sponsored by OpenAI.
- **High Quality.** For many video games, the data is stored in a well-organized data structure. Except for rare cases of game bugs, the data can be considered correct and accurate. We can hardly find missing or misrecorded values, which may be common in a real-world dataset.
- **High Completeness.** For a bird migration dataset, we may find much contextual information not recorded. For example, the birds may consider where there is a lake so that they can drink water. However, we cannot guarantee that all bird migration datasets record the position of each water source along the migration route. In contrast, the video game dataset is complete. Almost all the information that motivates the players' movements is recorded, except their mental activity. Thanks to this point, we recorded hundreds of contextual data states in our video game dataset, which greatly tested the capabilities of our model.

**B.1.2 Data Description.** We provide our code for downloading and preprocessing the dataset in our code repository. Finally, our dataset considered 99 game units and 273 contextual data states, shown as follows.

**Game Units.** Shown as Table 7, the set  $U$  includes 99 game units in total. Note that although some game units are static, we record their trajectories as POIs to improve the interpretability of our model, inspired by Bartoli et al. [3] who involving static obstacles into the trajectory prediction of pedestrian.

**Table 7: All the game units in  $U$ .**

Game Unit	Counts	Static or Moveable
Heroes controlled by players	$2 \times 5$	Moveable
Couriers	$2 \times 5$	
Lane Creeps (at the front)	$2 \times 3$	
Roshan	1	
Towers	$2 \times 11$	Static
Barracks	$2 \times 6$	
Base	2	
Outposts	2	
Runes	4	
Neutral Creeps Camps	16	
Ward Spots	14	

**Contextual data states.** Shown as Table 9, each data frame includes 283 data states. According to how players observe these data states, we classify them into three types, which determine how we record the value.

**Table 8: All the data states considered as context data.**

Value Types	Data States	Normalization Params	Note
Consensus data states are always known by all players			
Ranged	38 × Health of buildings	MIN=0, MAX=3000	The health points of different buildings are also different. However, all are below 3000.
Unlimited	Current time	$\hat{MAX}=2400s$	
	10 × Respawn time of heroes	$\hat{MAX}=60s$	
Boolean	Circadian state	0: daytime, 1: nighttime	
	10 × Survival states of heroes	0: alive, 1: dead	
	38 × Survival states of buildings	0: alive, 1: dead	
	2 × Which team controls the out-posts	0: Radiant, 1: Dire	
Categorical	10 × Heroes picked	embedding vector, $LE = 5$	
	10 × Roles	one-hot vector, $LE = 10$	
Vision-based data states are updated only when they can be observed by $p$			
Ranged	10 × Current positions of heroes	MIN=(8240,8220), MAX=(24510,24450)	Actually, a position can be regarded as two ranged numbers. For convenience, we regard it as one data state.
	10 × Current positions of couriers	same as above	
	10 × Positions of wards	same as above	
	10 × Levels of heroes	MIN=1,MAX=30	
Unlimited	10 × Health of heroes	$\hat{MAX}=3000$	
	10 × Mana of heroes	$\hat{MAX}=1700$	
	10 × Gold of heroes	$\hat{MAX}=15000$	
	Health of Roshan	$\hat{MAX}=4000$	
Boolean	2 × Existence of power runes	0: without, 1: with	
Categorical	2 × Power rune types	one-hot vector, $LE = 7$	
	60 × Items purchased	embedding vector, $LE = 7$	
Knowledge-based data states are updated when the data states are observable and can be known by players using their knowledge			
Ranged	6 × Positions of lane creeps	same as the positions mentioned above	Knowledge: The lane creeps move on certain paths.
	Position of Roshan	same as above	Knowledge: Roshan will be respawned at a fixed place.
Boolean	Survival state of Roshan	0: alive, 1: dead	Knowledge: There will be a broadcast when it is dead, and it must be respawned 12 minutes after its last death.
	2 × Existence of bounty runes	0: without, 1: with	Knowledge: Every three minutes
	2 × Existence of water runes	0: without, 1: with	Knowledge: At the 2nd and 4th minutes
	16 × Existence of neutral creeps	0: without, 1: with	Knowledge: At the start of every minute

## B.2 Bird

We constructed two datasets based on an open bird migration dataset [16]. According to the number of contextual data states, we named the two datasets as *Bird-2* and *Bird-8*, respectively. Note that we set  $|U|$  as 1 because the dataset did not record many birds' locations simultaneously.

*Bird-8* preserves eight contextual data states most relevant to birds' migratory trajectories. For some data states, we were not sure whether it is reasonable to classify them into the current types (e.g., regard temperature as a ranged data state). But this is supposed to have little influence on our model.

*Bird-2* only preserves two time-related contextual data states, namely, the timestamp and the season.

**Table 9: All the data states considered as context data.**

Value Types	Data States	Normalization Params	Note
Ranged	surface temperature	Min=250, MAX=320	May be in Kelvin.
	air temperature	Min=250, MAX=320	The average air temperature is between 400m and 1000m.
	surface pressure	MIN=97000, MAX=105000	
	timestamp	MIN=0, MAX=525600	Considering that bird migration takes a year as a cycle, we convert the timestamp into the ordinal number of minutes in each year, obtaining a ranged data state from 0 to $365 * 24 * 60$ .
Unlimited	wind speed in x direction	$\hat{MAX}=11$	
	wind speed in y direction	$\hat{MAX}=8$	
	bird density	$\hat{MAX}=6$	The vertically integrated bird density
Boolean	season	0: Spring, 1: Autumn	Birds usually migrate at these two seasons. The original dataset does not have data in the other two seasons.



## C COMPLETE EXPERIMENTS RESULTS

### C.1 Comparative Experiment I

**Table 10: The ADE loss of ten-round experiments on DOTA.**

Model	Round 0	Round 1	Round 2	Round 3	Round 4	Round 5	Round 6	Round 7	Round 8	Round 9	MEAN	SD
LSTM	1476.79	1393.91	1495.63	900.35	1185.02	1187.28	1048.58	1203.04	1555.00	1347.27	1279.29	199.89
Trans	1080.47	1222.13	1316.80	1053.44	1027.95	1317.84	1224.36	1420.34	1243.66	1370.29	1227.73	128.74
Tjf	1172.08	936.51	876.07	920.63	905.60	1061.73	1060.32	1030.19	861.18	869.66	969.40	99.73
DATF	749.47	867.41	724.00	1011.85	591.48	798.94	721.36	838.30	851.53	959.48	811.38	116.48
IETP-10	723.15	809.29	593.37	603.25	497.87	839.06	570.39	621.59	540.13	456.66	625.48	120.66
IETP-20	479.89	524.78	615.08	489.99	605.00	574.85	583.03	579.90	502.46	614.51	556.95	49.95
CATP-10	567.74	657.37	636.25	650.59	440.55	444.40	554.02	651.52	486.70	548.33	563.74	80.61
CATP-20	442.69	476.61	434.66	364.47	385.90	408.36	433.83	399.40	451.29	463.97	426.12	33.87
CATP-10-Tjf	525.01	569.00	623.32	479.20	525.51	635.43	553.09	428.19	521.44	521.29	538.15	58.61
CATP-20-Tjf	410.35	414.58	442.17	453.31	401.12	415.52	495.63	333.98	449.04	417.91	423.36	36.94

**Table 11: The ADE loss of ten-round experiments on Bird-8.**

Model	Round 0	Round 1	Round 2	Round 3	Round 4	Round 5	Round 6	Round 7	Round 8	Round 9	MEAN	SD
LSTM	23.99	19.33	17.21	23.65	19.08	19.13	19.26	25.81	25.85	18.93	21.22	3.06
Trans	21.97	18.41	18.21	18.46	23.74	18.42	22.21	24.74	16.79	23.81	20.68	2.76
Tjf	18.20	21.81	17.28	16.70	19.67	22.80	17.16	20.52	19.81	20.38	19.43	1.95
DATF	15.98	13.99	16.03	16.86	16.28	15.08	17.30	15.26	15.97	16.25	15.90	0.89
IETP-10	17.25	18.13	16.27	16.85	15.43	16.75	15.47	16.46	15.59	16.19	16.44	0.81
IETP-20	15.91	13.14	13.09	13.78	14.56	12.65	14.46	12.41	12.68	15.09	13.78	1.12
CATP-10	10.93	11.60	12.16	12.51	12.31	12.01	11.72	12.09	12.39	11.65	11.94	0.45
CATP-20	17.20	15.93	19.52	19.22	17.20	16.19	14.76	16.21	16.59	17.97	17.08	1.41
CATP-10-Tjf	11.67	12.92	12.22	9.68	12.34	12.04	12.09	12.92	12.95	10.59	11.94	1.01
CATP-20-Tjf	20.49	17.48	20.31	18.84	19.28	20.28	14.81	16.44	18.65	16.95	18.35	1.80

**Table 12: The ADE loss of ten-round experiments on Bird-2.**

Model	Round 0	Round 1	Round 2	Round 3	Round 4	Round 5	Round 6	Round 7	Round 8	Round 9	MEAN	SD
LSTM	24.49	24.28	28.95	16.71	21.21	17.37	21.89	28.86	19.81	30.55	23.41	4.63
Trans	22.85	26.99	26.09	24.55	23.91	24.32	21.01	21.21	26.22	27.01	24.42	2.10
DATF	17.91	15.75	14.95	16.27	16.11	17.36	17.58	17.13	16.64	16.69	16.64	0.86
IETP-10	18.63	17.53	20.50	20.75	20.54	22.41	22.22	19.53	21.15	19.48	20.27	1.44
IETP-20	17.56	17.92	16.68	17.95	14.84	16.40	18.04	19.80	17.50	21.05	17.77	1.64
CATP-10	15.28	15.13	17.79	20.90	18.31	22.32	19.27	14.22	13.90	20.25	17.74	2.83
CATP-20	20.52	27.77	27.57	24.69	22.28	21.59	22.67	19.93	21.91	24.21	23.31	2.58
CATP-10-Tjf	18.21	16.31	18.64	21.20	18.02	16.34	11.53	17.77	18.64	15.92	17.26	2.40
CATP-20-Tjf	21.55	15.93	21.66	18.01	22.48	25.40	22.03	15.79	25.48	23.85	21.22	3.36

*\*Note: Since Tjf accepted only TX as the input, it was unnecessary to repeat the experiments for Tjf on Bird-2.*

## C.2 Comparative Experiment II

**Table 13: The MSE loss of ten-round experiments on SP.**

Model	Round 0	Round 1	Round 2	Round 3	Round 4	Round 5	Round 6	Round 7	Round 8	Round 9	MEAN	SD
LSTM	5.43	5.91	4.97	5.28	5.72	6.15	6.56	4.98	5.40	6.46	5.69	0.54
Trans	5.85	5.25	5.08	5.85	5.23	6.96	5.03	5.67	6.17	4.67	5.57	0.63
Informer	4.48	5.77	4.52	3.97	4.33	5.35	6.62	4.77	4.11	4.17	4.81	0.81
Autoformer	2.70	3.29	3.45	3.22	3.84	3.10	2.81	3.16	2.99	3.06	3.16	0.31
FEDformer	3.12	2.81	3.92	3.36	2.97	2.99	2.76	3.15	3.34	3.13	3.16	0.32
TimesNet	2.97	3.06	2.73	2.98	3.16	3.16	2.48	2.62	2.90	3.22	2.93	0.23
MW-LSTM	5.27	4.02	4.96	4.42	5.03	5.13	4.84	5.25	4.58	5.13	4.86	0.39
MW-Trans	4.52	4.70	4.70	5.89	3.85	4.42	5.49	4.86	4.17	4.81	4.74	0.56
MW-TN	2.90	2.70	2.78	3.01	2.84	3.05	2.91	2.84	2.61	2.92	2.86	0.13

**Table 14: The MSE loss of ten-round experiments on ET.**

Model	Round 0	Round 1	Round 2	Round 3	Round 4	Round 5	Round 6	Round 7	Round 8	Round 9	MEAN	SD
LSTM	1.25	1.44	1.59	1.19	1.43	1.36	1.46	1.32	1.52	1.38	1.40	0.12
Trans	1.28	1.38	1.31	1.24	1.05	1.03	1.39	1.23	1.09	1.31	1.23	0.13
Informer	1.26	1.03	0.95	0.81	1.11	1.07	1.05	0.98	1.16	1.01	1.04	0.12
Autoformer	0.48	0.53	0.53	0.52	0.44	0.53	0.53	0.46	0.56	0.41	0.50	0.05
FEDformer	0.48	0.49	0.46	0.48	0.42	0.53	0.52	0.41	0.39	0.42	0.46	0.05
TimesNet	0.60	0.42	0.47	0.46	0.41	0.47	0.42	0.48	0.48	0.45	0.47	0.05
MW-LSTM	0.86	1.01	0.89	0.82	0.89	1.09	1.05	1.11	1.10	1.06	0.99	0.10
MW-Trans	1.09	0.97	1.09	0.89	0.94	1.11	1.16	0.76	0.99	1.04	1.00	0.11
MW-TN	0.51	0.48	0.39	0.45	0.46	0.45	0.46	0.43	0.36	0.50	0.45	0.04